Appl. Phys. B 62, 173–182 (1996)

Applied Physics B Lasers and Optics

Minimization of cavitation effects in pulsed laser ablation illustrated on laser angioplasty

A. Vogel[1,*], R. Engelhardt[1], U. Behnle[1], U. Parlitz[2]

[1] Medical Laser Center Lübeck, Peter-Monnik-Weg 4, D-23562 Lübeck, Germany
(Fax: + 49-451/505486)
[2] Third Physics Institute, University of Göttingen, Bürgerstrasse 42–44, D-37073 Göttingen, Germany
(Fax: + 49-551/397720)

Received: 8 March 1995/Accepted: 14 June 1995

Abstract. Cavitation effects in pulsed laser ablation can cause severe deformation of tissue near the ablation site. In angioplasty, they result in a harmful dilatation and invagination of the vessel walls. We suggest to reduce cavitation effects by dividing the laser pulse energy into a pre-pulse with low and an ablation pulse with high energy. The pre-pulse creates a small cavitation bubble which can be filled by the ablation products of the main pulse. For suitable energy ratios between the pulses, this bubble will not be enlarged by the ablation products, and the maximal bubble size remains much smaller than after a single ablation pulse. The concept was analyzed by numerical calculations based on the Gilmore model of cavitation dynamics and by high-speed photography of the effects of single and double pulses performed with a silicone tube as vessel model. The use of double pulses prevents the deformation of the vessel walls. The concept works with an energy ratio of up to about 1:30 between the pulses. For the calculated optimal ratio of 1:14.6, the bubble volume is reduced by a factor of 17.7. The ablation pulse is best applied when the pre-pulse bubble is maximally expanded, but the timing is not very critical.

PACS: 62.50. + p; 79.20.Ds; 87.00

In various fields of pulsed laser surgery, e.g., laser angioplasty, orthopaedics, laser lithotripsy, and ophthalmology, the ablation, fragmentation, or disruption process takes place in a liquid environment. Pulsed laser ablation is here always accompanied by cavitation, which does not occur at a tissue–air interface. Cavitation leads to structural deformation of the adjacent tissue, which is often undesirable and can be more pronounced than the ablative tissue effect itself [1, 2]. We studied the role of cavitation and developed a concept to minimize cavitation-induced damage. This concept is illustrated on laser angioplasty, but it is generally applicable to pulsed laser ablation in a liquid environment.

In pulsed laser angioplasty, ablation goes along with an explosive evaporation process in the blood-filled vessel. This generates a cavitation bubble [3, 4] whose expansion leads to a microsecond dilatation of the vessel wall [5]. The subsequent bubble collapse leads to an invagination of the vessel wall which further adds to the mechanical trauma [6]. It is likely that the mechanical damage and the subsequent healing response contribute to the relatively high rate of re-stenosis observed after laser angioplasty [7–12], which has prevented a widespread clinical acceptance of the method. Litvack et al. [13] and Tcheng et al. [14] proposed flushing of the arteries with saline to reduce the absorption of excimer-laser light by blood and thus diminish cavitation. Oberhoff et al. [15] suggested to divide the energy of one excimer-laser pulse both spatially and in time into 8 smaller pulses ("multiplexing"), which also diminishes cavitation. Both concepts can, however, only lead to a gradual decrease of the cavitation effects, because they do not avoid ablation taking place in a liquid surrounding.

The most consequent approach to avoid cavitation is to displace the liquid from the vicinity of the ablation site. We accomplished this without an injection of an exogenous gas by dividing the laser-pulse energy into a pre-pulse with low energy and an ablation pulse with higher energy. The pre-pulse creates a small cavitation bubble, and the ablation pulse is applied when this bubble is maximally expanded and can be filled by the ablation products of the main pulse. The energy of the pre-pulse must be small enough to keep the cavitation effects below the damage threshold of the vessel walls. If the energy ratio of both pulses is chosen appropriately, the ablation products will not lead to a further expansion of the bubble generated by the pre-pulse, and the maximal bubble size will remain much smaller than after a single ablation pulse.

To identify a suitable ratio between the pre-pulse and the ablation pulse, and to analyze how critical the timing between the pulses is, we performed numerical calculations of the temporal development of the bubble radius and the pressure inside the bubble. The experimental analysis of the cavitation effects after single and double

* To whom all correspondence should be addressed

laser pulses was done in vitro with a silicone tube immersed in water as vessel model. Double pulses with variable energy ratio and time separation were realized by coupling the output of two lasers into the same quartz fiber. The laser-induced events were documented by high-speed photography at 50 000 frames/s.

1 Numerical calculations

For the calculation of the temporal development of the bubble radius and the pressure inside the bubble, we used the Gilmore model of cavitation-bubble dynamics [16, 17] which takes into account the compressibility of the liquid surrounding the bubble, viscosity, and surface tension. Thereby, the consideration of compressibility is most important; viscosity and surface tension are of little significance for the experimental conditions discussed in this paper [17]. The model originally assumes a constant gas content of the bubble, given by its equilibrium radius. We modelled the bubble expansion in pulsed laser ablation by introducing a time-dependent equilibrium radius which reflects the evaporation of water, tissue and plaque by the laser pulse.

The dynamics of a spherical cavitation bubble is described by the equation

$$\dot{U} = \left[-\frac{3}{2}\left(1 - \frac{U}{3C}\right) U^2 + \left(1 + \frac{U}{C}\right) H + \frac{U}{C}\left(1 - \frac{U}{C}\right) R \frac{dH}{dR} \right] \left[R\left(1 - \frac{U}{C}\right) \right]^{-1}. \tag{1}$$

Here, R is the radius of the bubble, $U = dR/dt$ the bubble wall velocity, C the speed of sound in the liquid at the bubble wall, and H the enthalpy difference between the liquid at the bubble wall and at infinity:

$$H = \int_{p_{\text{stat}}}^{P(R)} \frac{dp}{\rho}. \tag{2}$$

P is the pressure at the bubble wall, p_{stat} the hydrostatic pressure, ρ and p are the density and pressure within the liquid, respectively. The pressure at the bubble wall is given by

$$P(R, U) = \left(p_{\text{stat}} + \frac{2\sigma}{R_n}\right)\left(\frac{R_n}{R}\right)^{3\kappa} - \frac{2\sigma}{R} - \frac{4\mu}{R} U. \tag{3}$$

R_n is the equilibrium radius of the bubble, i.e., the radius where the pressure inside the bubble equals the hydrostatic pressure. R_n is thus a measure of the gas content of the bubble. When the equation of state of water is approximated by the (empirical) Tait equation with $B = 295.5$ MPa and $n = 7$

$$\frac{P(R, U) + B}{p_{\text{stat}} + B} = \left(\frac{\rho}{\rho_0}\right)^n, \tag{4}$$

one obtains the following relationships for the enthalpy H and the sound velocity C at the bubble wall:

$$C = [c_0^2 + (n-1)H]^{1/2},$$
$$H = \frac{n(p_{\text{stat}} + B)}{(n-1)\rho_0}\left[\left(\frac{P + B}{p_{\text{stat}} + B}\right)^{(n-1)/n} - 1\right]. \tag{5}$$

For water at a temperature of 20°C, the constants in the above equations are: density of water $\rho_0 = 998\ \text{kg/m}^3$, surface tension $\sigma = 0.072583$ N/m, polytropic exponent $\kappa = 4/3$, coefficient of the dynamic shear viscosity $\mu = 0.001046\ \text{Ns/m}^3$, velocity of sound $c_0 = 1483$ m/s, and static ambient pressure $p_{\text{stat}} = 100$ kPa.

When the initial bubble radius R_0 is larger than the equilibrium radius R_n, the pressure inside the bubble is lower than the hydrostatic pressure, and the bubble collapses. When, on the other hand, the initial bubble radius is smaller than R_n, the pressure inside the bubble is high, and the bubble expands. This gives a clue for the modelling of the bubble expansion in pulsed laser ablation by a time-dependent equilibrium radius [18]. The deposition of laser-light energy can be simulated by raising R_n from a small initial value R_{na} to a much larger final value R_{nb}. The radius R_{na} of the bubble nucleus at time $t = 0$ is identified with the liquid volume evaporated by the laser pulse. It is assumed that the volume increase $(4/3\pi)(R_{nb}^3 - R_{na}^3)$ of the equilibrium bubble during the laser pulse is proportional to the pulse energy E_L resulting in evaporation:

$$\frac{4}{3}\pi(R_{nb}^3 - R_{na}^3) \propto E_L = \int_0^{2\tau} P_L\, dt. \tag{6}$$

Here, P_L denotes the laser power, and 2τ the total laser pulse duration. R_{nb} was chosen to yield a maximal bubble radius similar to that experimentally observed during excimer-laser angioplasty. The corresponding R_{na} values were obtained by dividing R_{nb} by the volume expansion coefficient $\Omega = 1662$ of water for evaporation at equilibrium conditions [19]:

$$R_{na} = R_{nb}/\Omega. \tag{7}$$

The adjustment of R_{nb} and R_{na} to the maximal radius of the cavitation bubble produced by the laser pulse links these variables to an easily measurable parameter which "summarizes" the preceding ablation dynamics. This circumvents a detailed analysis of the evaporation process, which would be required to determine R_{nb} from the fraction of the incident laser-pulse energy contributing to evaporation and bubble formation.

The temporal shape of the laser pulse is modelled by a $\sin^2$ function with duration τ (FWHM), and total duration 2τ (Fig. 1):

$$P_L(t) = \sin^2\left(\frac{t}{2\tau}\pi\right), \quad 0 \le t \le 2\tau. \tag{8}$$

With the assumptions (6) and (8), we obtain the following expression for the temporal development of R_n during the laser pulse:

$$R_n(t) = \left\{ R_{na}^3 + \frac{R_{nb}^3 - R_{na}^3}{2\tau}\left[t - \frac{\tau}{\pi}\sin\left(\frac{\pi}{\tau}t\right)\right]\right\}^{1/3}. \tag{9}$$

The bubble formation after double pulses is modelled by increasing R_n in two steps separated by the time interval Δt between the pulses (Fig. 1). With (6), the ratio ε of the evaporation energies provided by the pre-pulse and the ablation pulse is given by the ratio of the volume

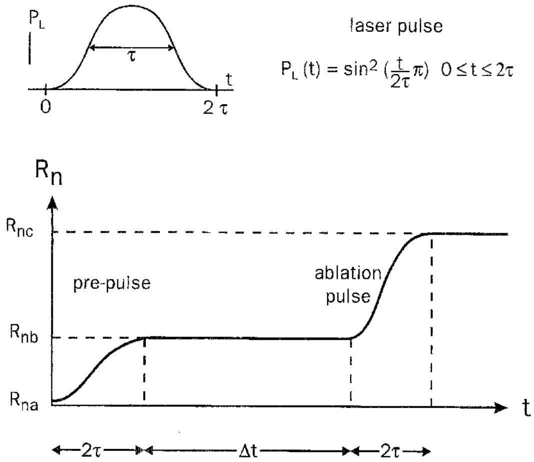

Fig. 1. Model of the energy input into a small cavitation bubble nucleus by a pre-pulse and a subsequent ablation pulse. Each pulse is described by a $\sin^2$ function with duration τ (FWHM) and total duration 2τ. The pulses are separated by the time interval Δt. The equilibrium radius R_n of the bubble is increased in two steps according to (9) and (11)

increase of the equilibrium radius after each pulse:

$$\varepsilon = \frac{R_{nb}^3 - R_{na}^3}{R_{nc}^3 - R_{nb}^3}. \tag{10}$$

The ratio ε of the evaporation energies equals the ratio of the respective laser-pulse energies if the fraction of the laser energy resulting in evaporation is the same for both pulses. This conditions is probably fulfilled at energy values well above the ablation threshold, but most likely not near threshold.

The increase of R_n during the pre-pulse is described by (9), and the rise of R_n during the ablation pulse is given by

$$R_n(t) = \left\{ R_{nb}^3 + \frac{R_{nc}^3 - R_{nb}^3}{2\tau}\left[t - \Delta t - \tau - \frac{\tau}{\pi}\sin\left(\frac{\pi}{\tau}t\right)\right]\right\}^{1/3}. \tag{11}$$

For solving the differential equation (1), it has been rewritten as a system of first-order differential equations and integrated numerically with a predictor–corrector method [20]. We calculated $R(t)$ and $P(t)$ for various values of the energy ratio and the time separation between pre-pulse and ablation pulse.

2 Experiments

The experimental analysis was performed in vitro with a silicone tube immersed in water as vessel model. The tube had 5 mm diameter, and the wall thickness was 0.4 mm. The mechanical properties were similar to those of human arteries: Young's modulus was measured to be 2 N/mm^2, whereas it is 2–5 N/mm^2 for vessels [21]. The silicone tube was filled with water instead of blood to enable visualization of the cavitation-bubble dynamics. The laser pulses were delivered via a 275 μm quartz fiber onto a dark stone target modelling calcified plaque, which guaranteed energy absorption under reproducible conditions. An injection needle guiding the fiber was used to position the fiber tip inside the silicone tube.

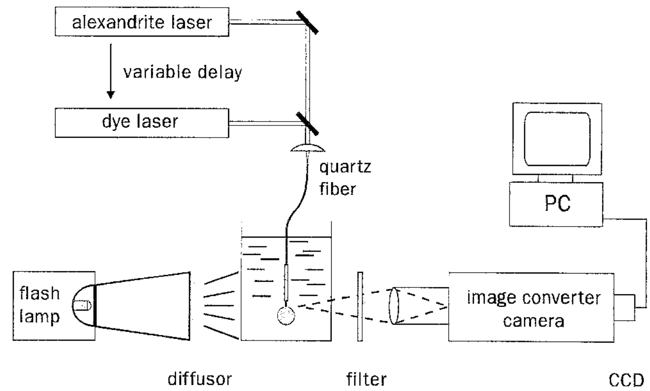

Fig. 2. Experimental set up for high-speed photography of the cavitation effects during pulsed laser angioplasty

The experimental setup for the investigation of cavitation effects is depicted in Fig. 2. Double pulses with variable energy ratio and time separation were generated by coupling the output of two lasers into the quartz fiber. The ablation pulse was produced by a flash-lamp-pumped dye laser (Vuman, PDL-20) delivering pulses with 3 μs duration at a wavelength of 630 nm, and the pre-pulse was generated with a Q-switched alexandrite laser (Light Age, PAL 101) delivering pulses with a duration of 120 ns and a wavelength of 750 nm. The laser-induced events were documented by high-speed photography with an image-converter camera (Hadland Photonics, Imacon 792) at a framing rate of 50 000 frames/s. Either a Polaroid 667 (3000 ASA) film or a CCD camera (Hamamatsu C3077) were used as recording medium. We took picture series of 8 frames each. To enlarge the time of observation, several picture series with the same laser parameters and different starting times were sometimes combined to a longer sequence. The acoustic transients emitted during the generation and oscillation of the cavitation bubbles were measured using a PVDF hydrophone (CERAM miniature hydrophone) with a rise time of 12 ns.

We investigated the cavitation effects after a single ablation pulse with an energy of 70 mJ and after double pulses where the ablation pulse with 70 mJ pulse energy was applied after the bubble generated by a 10 mJ pre-pulse had expanded to its maximal size. First, we studied the deformation of the silicone tube by the cavitation bubble dynamics. In a second series of experiments, we investigated how much the cavitation-bubble radius can be reduced by adding the pre-pulse to the ablation pulse, and how much this decrease depends on the time interval between the pulses. For these measurements, the stone target was placed in a water-filled container to avoid any disturbance of the bubble dynamics by the silicone tube. A number of picture series with increasing time delay between the laser pulses was taken, and from each series the maximal bubble radius was determined. On the whole, 250 picture series were taken, 6 series for each time delay. They were recorded with the CCD camera attached to the image-converter camera and displayed on a video monitor. The maximal bubble radius was determined from the monitor.

3 Results

3.1 Calculations

Figure 3 shows the calculated cavitation bubble dynamics for a) a single ablation pulse, b) the pre-pulse, and c) both pulses separated by a time interval of 70 μs. This is the time after which the pre-pulse bubble is maximally expanded. The energy ratio between the pulses is 1:14.6. The R_n value at the end of the ablation pulse was chosen such that the maximal radius of the bubble is approximately the same as observed by van Leeuwen et al. [6] when 14 mJ excimer-laser pulses were delivered into a haemoglobin solution. The laser-pulse duration was set to 120 ns (FWHM), which is a typical pulsewidth for clinically used XeCl-excimer lasers [5, 6] and at the same time the pulse duration of the alexandrite laser used in our experiments. With the ablation pulse alone, the maximum bubble radius is 1.93 mm (Fig. 3a), as compared to 0.75 mm with the pre-pulse alone (Fig. 3b). During the application of the ablation pulse, the pressure inside the bubble rises for less than a microsecond to 580 MPa. The large pressure inside the cavity accelerates the surrounding liquid, and, because of the inertia of the fluid mass, the bubble expands beyond the point where the inner pressure equals the hydrostatic pressure. The pressure inside the bubble is therefore far below the hydrostatic pressure during most of the bubble oscillation time. The low pressure inside the expanded bubble leads to its collapse, whereby the bubble content is compressed, and the pressure rises again to 62 MPa. Therefore, the bubble rebounds, and the oscillation cycle repeats itself. The bubble oscillations are damped, because during each bubble collapse an acoustic transient is radiated into the surrounding liquid [22]. When the ablation pulse is fired into the expanded pre-pulse bubble (Fig. 3c), the bubble radius remains constant at 0.75 mm, with minute oscillations around the equilibrium value R_{nc}. The pressure inside the pre-pulse bubble is raised to hydrostatic pressure and remains constant, with only slight fluctuations (<0.01 MPa) around this value. The increased amount of gas inside the bubble produced by the ablation pulse prevents its collapse, and hence there is no pressure transient originating from collapse. In reality, the bubble content would condense or dissolve in the liquid

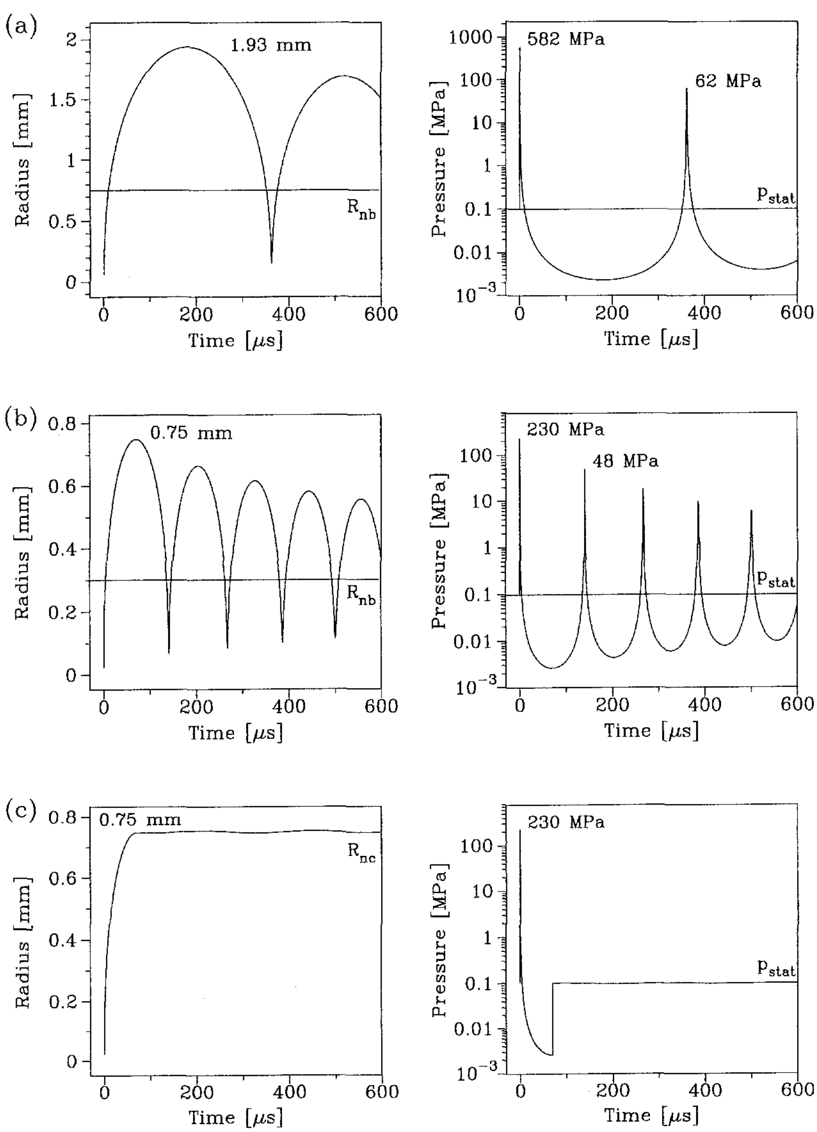

Fig. 3a–c. Calculated dynamics of laser-generated cavitation bubbles. **a** Bubble radius $R(t)$ (*left*) and pressure $P(t)$ (*right*) inside the bubble after the ablation pulse alone (R_{na} = 63 μm, R_{nb} = 750 μm); **b** Dynamics after the pre-pulse alone (R_{na} = 25 μm, R_{nb} = 300 μm); **c** Ablation pulse applied 70 μs after the pre-pulse, when the pre-pulse bubble is maximally expanded (R_{na} = 25 μm, R_{nb} = 300 μm, R_{nc} = 750 μm). The duration of each pulse is 120 ns. The energy ratio between pre-pulse and ablation pulse is 1:14.6

after some time, and the bubble would disappear. This cannot be portrayed by the Gilmore model, because it neglects condensation and gas diffusion. The maximal bubble volume after double pulses is smaller by a factor of 17.7 than that after the ablation pulse alone.

When the energy ratio is larger than in the optimal case described above, the ablation pulse raises the pressure inside the pre-pulse bubble above hydrostatic pressure, and the bubble starts to grow again. With a ratio of 1:36 (Fig. 4), the pressure rises to 0.3 MPa and the maximal bubble volume after the application of double pulses is only by a factor of 8.5 smaller than after the ablation pulse alone – as compared to a factor of 17.7 in the optimal case.

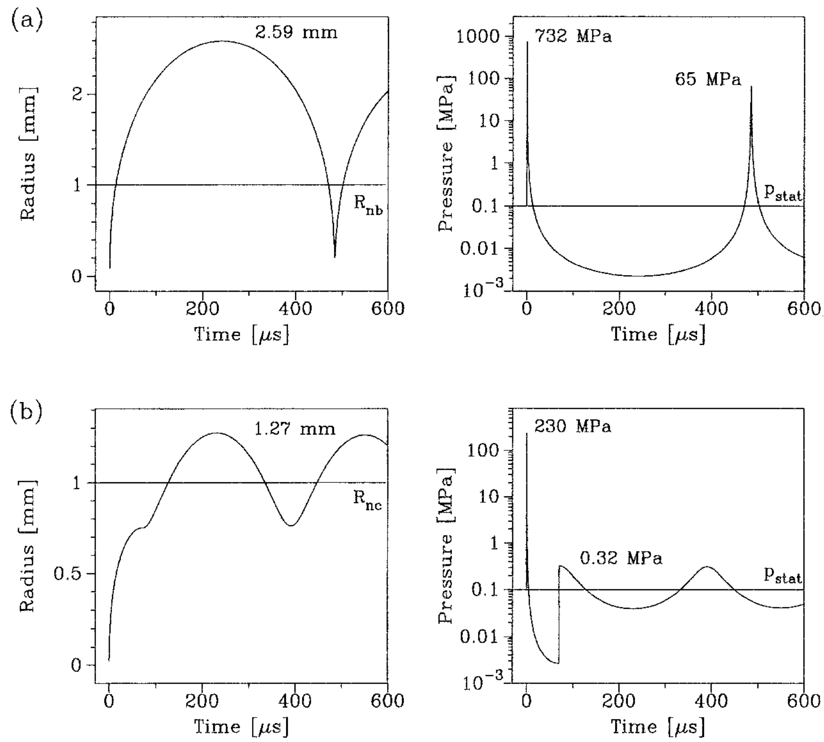

Fig. 4a, b. Calculated bubble radius $R(t)$ (*left*) and pressure $P(t)$ (*right*) inside the bubble when the energy ratio between pre-pulse and ablation pulse is 1:36. (**a**) Ablation pulse alone ($R_{na} = 85$ μm, $R_{nb} = 1000$ μm); (**b**) Ablation pulse applied 70 μs after the pre-pulse ($R_{na} = 25$ μm, $R_{nb} = 300$ μm, $R_{nc} = 1000$ μm). The pre-pulse is the same as in Fig. 3. The duration of each pulse is 120 ns

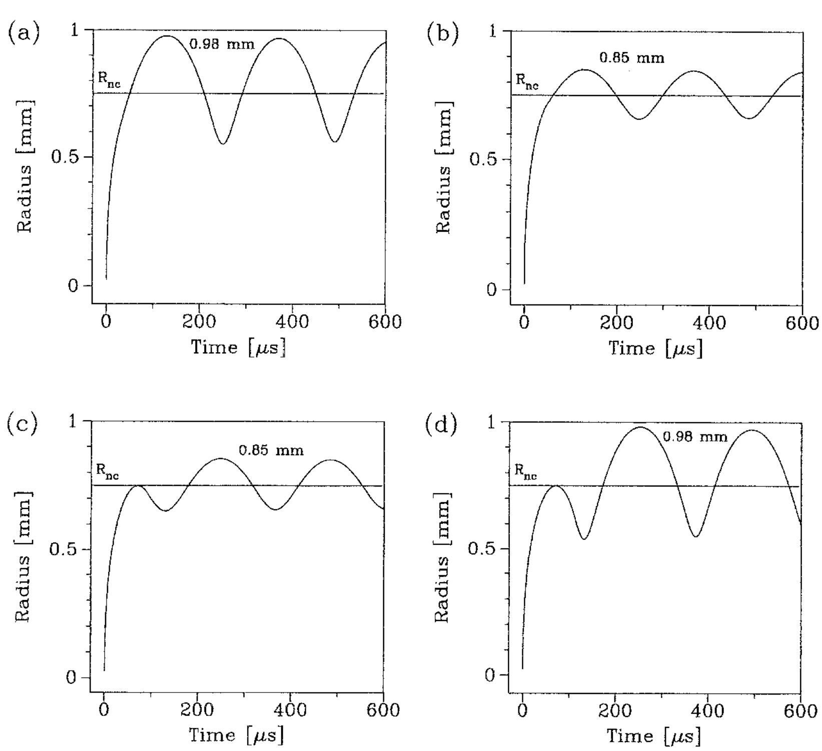

Fig. 5a–d. Calculated bubble radius R after the application of double pulses with various time delays between pre-pulse and ablation pulse. The time delay is (**a**) 30 μs; (**b**) 50 μs; (**c**) 90 μs; (**d**) 110 μs. The other parameters are the same as in Fig. 3

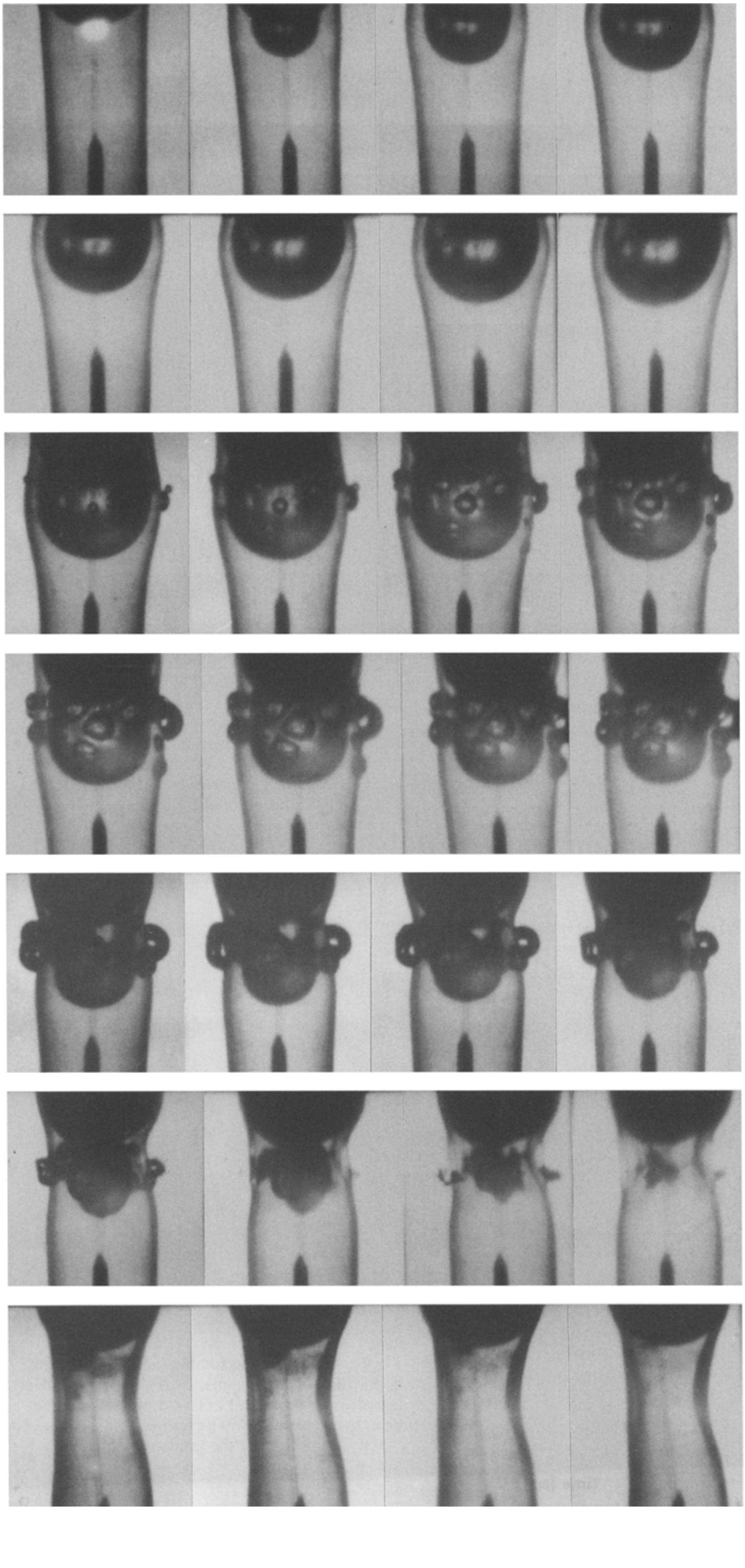

Fig. 6. Dilatation and invagination of the silicone tube after a 70 mJ dye-laser pulse with 3 μs duration. The fiber is in contact with the stone. The interframing time is 20 μs, and the diameter of the non-dilated tube is 5 mm (see text)

Maximal radius reduction is achieved when the ablation pulse is released at maximal expansion of the pre-pulse bubble (Fig. 3c). When the ablation pulse is fired 20 μs earlier or later (Figs. 5b, c), the bubble dynamics does, however, not differ considerably from the optimal case. Even when the timing is 40 μs away from the optimum (Figs. 5a, d), the pressure inside the pre-pulse bubble does not rise to more than 3 bar above the hydrostatic pressure, and the maximal bubble volume is still by a factor of 8 smaller than after a single ablation pulse.

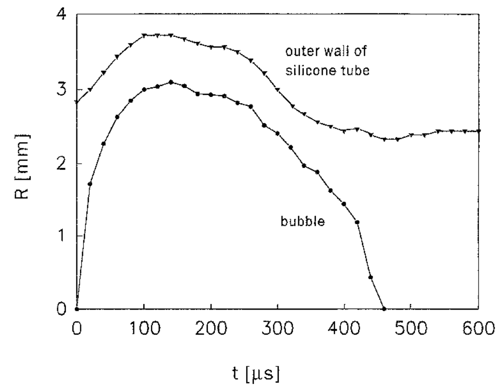

Fig. 7. Radius–time curve of the bubble inside the silicone tube and of the tube near the application site, measured from the picture series in Fig. 6. At $t = 0$, the radius of the tube is slightly larger than 2.5 mm (nominal tube diameter) because of the stone target inside

3.2 Experiments

3.2.1 Single pulses. Figure 6 shows the cavitation events produced by a 70 mJ laser pulse. The bright spot in the first frame is a plasma flash at the surface of the stone target. The plasma-mediated explosive evaporation drives the expansion of a cavitation bubble which causes

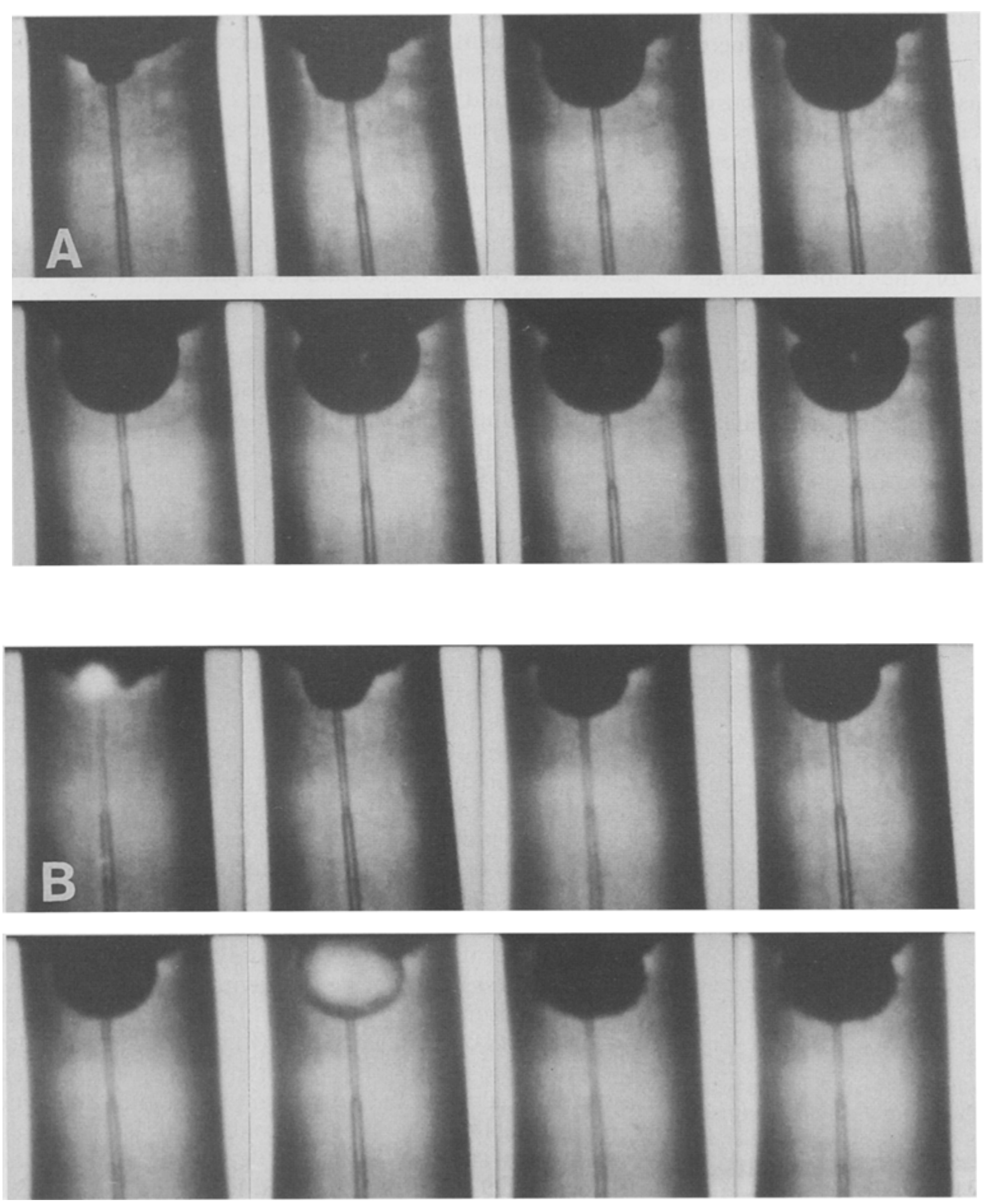

Fig. 8A, B. Reduction of cavitation effects by double pulses: (**A**) Pre-pulse alone, (**B**) pre-pulse and ablation pulse. The pre-pulse had an energy of 10 mJ and was delivered by an alexandrite laser ($\lambda = 750$ nm, $\tau = 120$ ns). The ablation pulse had 70 mJ pulse energy and was delivered by a dye laser ($\lambda = 630$ nm, $\tau = 3$ μs). The fiber was in contact with the stone. The interframing time is 20 μs, the tube diameter 5 mm. The ablation pulse was released 100 μs after the pre-pulse, when the bubble generated by the pre-pulse was maximally expanded. It did neither enlarge the pre-pulse bubble nor produce a dilatation of the tube. When the ablation pulse is applied alone (Fig. 6), it causes a marked dilatation and invagination a dilatation of the tube. Figure 7 shows the radius–time curves of the bubble and of the tube wall near the application site. The maximal dilatation is reached after about 120 μs and amounts to 135% of the initial tube diameter. The subsequent bubble collapse goes along with an invagination of the tube wall, whereby the minimal diameter is 82% of the original value. During the oscillation of the cavitation bubble in the silicone tube, cavitation bubbles also develop in the water *surrounding* the tube (Fig. 6). The cavitation bubbles outside the tube indicate the existence of a tensile stress wave which is strong enough to overcome the cavitation threshold in water.

3.2.2 Double pulses. Figure 8 shows the reduction of cavitation effects by double pulses. After a 10 mJ pre-pulse alone, no dilatation of the silicone tube is observed because the pulse energy is small. In Fig. 8b, a 70 mJ ablation pulse is released 100 μs after the pre-pulse, when the pre-pulse bubble is maximally expanded. The plasma flash of the ablation pulse is clearly visible in the sixth frame, but again no dilatation occurs, although the energy of the ablation pulse is the same as in Fig. 6. The maximal bubble radius after double pulses is about 1.6 mm, whereas it is 3.05 mm (within the dilated tube) after a single ablation pulse. Hydrophone measurements of the acoustic signal after double pulses showed only a pressure transient after the release of the pre-pulse, but no transients originating from the ablation pulse or the cavitation bubble collapse were detected. This is in accordance with the results of the calculations presented in Fig. 3c.

Figure 9 shows the ratio of the bubble Radius R_{1+2} after double pulses and the bubble radius R_2 after the ablation pulse alone, plotted as a function of the time separation of the pulses. The pulse energies were 10 mJ for the pre-pulse and 70 mJ for the ablation pulse. For zero delay between the pulses, no reduction of the radius is observed, as expected. The maximum reduction is achieved for a delay of 120 μs, which corresponds approximately to the time when the pre-bubble is maximally expanded (105 μs). In this case, the radius was lowered to 40% of the value reached without pre-pulse, and the volume was reduced by a factor of 15. When the time

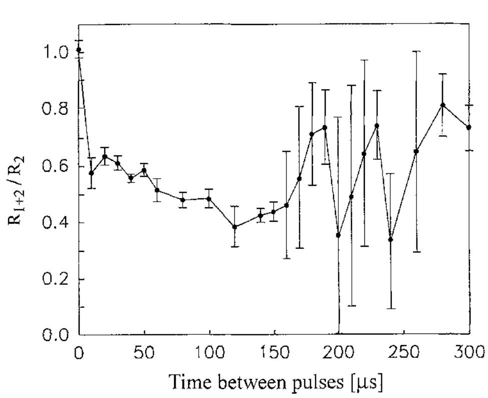

Fig. 9. Ratio between the bubble Radius R_{1+2} after double pulses and the bubble radius R_2 after the ablation pulse alone plotted as a function of the time separation of the pulses. The pulse energies were 10 mJ for the pre-pulse ($\lambda = 750$ nm, $\tau = 120$ ns) and 70 mJ for the ablation pulse ($\lambda = 630$ nm, $\tau = 3$ μs)

separation between the pulses is larger than 150 μs, the radius reduction decreases and varies strongly between different experiments, because at these times the ablation pulse is fired into the pre-pulse bubble shortly before or after its collapse (the collapse time of the pre-pulse bubble alone is 210 μs).

4 Discussion

4.1 Dynamics after single pulses

Our calculations indicate that during the initial phase after the laser exposure the pressure inside the cavitation bubble reaches hundreds of MPa (Fig. 3: 582 MPa, Fig. 4: 732 MPa). This is the origin of acoustic transients travelling into the surrounding liquid, whereby their initial pressure amplitude equals the pressure inside the bubble. Pressure amplitudes of up to 100 MPa were also observed experimentally by Esenaliev et al. [23] during excimer-laser ablation of aorta in an air environment. The values calculated for a liquid environment are higher because of the confinement of the laser-induced blowoff [24–26]. The large pressure inside the cavity accelerates the surrounding liquid and thus transforms the potential energy of the heated vapor into kinetic energy of the radial liquid flow. When the pressure inside the bubble falls to the ambient pressure, the driving force ceases, but the bubble continues to expand because of the inertia of the fluid mass: In an unbounded liquid, this leads to an enlargement of the bubble far beyond the equilibrium (Figs. 3a, b and 4), and in a vessel, it can lead to a dilatation of the vessel wall (Figs. 6, 7).

To estimate the energy spent on the dilatation of the silicone tube after a 70 mJ laser pulse, we compared the maximal bubble radius $R_{\max}$ in an unbounded liquid (3.8 mm, picture not shown) to the maximal bubble radius in the tube (3.05 mm, Fig. 7). The bubble energy is given by $E_B = 4/3\pi R_{\max}^3 \Delta p$. When the pressure difference Δp between inner and outer pressure is assumed to be close to 0.1 MPa (the hydrostatic pressure) in both cases, we obtain the result that 50% of the bubble energy is consumed in the dilatation process. The bubble energy in the unbounded liquid is 22 mJ, i.e., the dilatation energy is 11 mJ. The cavitation-induced tissue effects are more severe than the tissue effects caused by the pressure transients originating from the laser exposure. The latter remain on a cellular or subcellular level because of their short duration [1, 2, 27, 28]. In contrast to this, the work done by the expanding vapor cavity results in a structural deformation of the tissue on a much larger scale.

Dilatation of a vessel wall by an expanding cavitation bubble was already observed by van Leeuwen et al. [6]. A new observation made in our study is the occurrence of a tensile stress wave during the cavitation-bubble oscillation, which is indicated by the small cavitation bubbles on the *outer* wall of the silicone tube (Fig. 6). A lower limit for the amplitude of the stress wave is given by the fact that it must be larger than the cavitation threshold in the liquid surrounding the tube. The threshold for ultrasonic cavitation in tap water is 0.1–1.0 MPa depending on the sound frequency [29], and the threshold for cavitation induced by a single pressure transient of submicrosecond duration is 0.75–0.8 MPa [30, 31]. The tensile stress can be explained by the elastic rebound of the dilated tube or vessel wall, respectively. It may contribute to the histologic picture observed after laser angioplasty, namely medial dissections running parallel to the artery wall [6], because tissue is generally more susceptible to tensile stress than to pressure waves [21].

4.2 Dynamics after double pulses

The double-pulse technique makes it possible to displace the liquid near the ablation site without introducing any exogeneous gas into the vessel: cavitation is used to reduce the cavitation effects of the ablation pulse. The maximal bubble volume was lowered by a factor of 15 (experiments) and 17.7 (calculations), as compared to the case where only the ablation pulse is applied (Figs. 9, 3). Since at maximum expansion the pressure inside the pre-pulse bubble is far below the hydrostatic pressure, the bubble can be filled by the evaporated material from the ablation pulse without being further expanded. Thus, no additional kinetic energy is produced by the ablation pulse. The energy deposited is mainly dissipated by heat conduction, and, to a smaller part, by the acoustic transient emitted during bubble collapse. This transient is, however, weaker than after a single ablation pulse, because the increased amount of material inside the bubble slows down the collapse velocity of the bubble. On the whole, less energy is converted into mechanical forms (acoustic and kinetic energy of the fluid around the expanding bubble), and a higher percentage is directly dissipated as heat. This leads to a minimization of the mechanical trauma to adjacent tissue. Thermal tissue damage at the bubble wall should, however, also remain insignificant, because the pulse energies used are relatively small, and the ablation products cool down adiabatically during their expansion into the pre-pulse bubble.

4.2.1 Maximal radius reduction. The maximal radius reduction found experimentally is almost the same as that predicted by the numerical calculations. The radius is in both cases lowered to about 40% of the original value and the bubble volume to 7%. This agreement between calculations and experiment should, however, not be overestimated, because the small ablation rate of the stone used as a target and the plasma-mediated ablation process do not necessarily correspond to the assumptions made in the calculations (evaporation of material proportional to the laser pulse energy). The energy ratio yielding maximal radius reduction was 1:14.6 in the calculations and 1:7 in the experiments. It should be noted that the calculations refer to the energy resulting in evaporation of the ablated material, whereas the experimental values apply to the total laser pulse energy at the fiber tip, which does not completely contribute to evaporation. Near threshold, the percentage of energy leading to evaporation is smaller than at higher pulse energy. The ratio of the *effective* pre-pulse and ablation-pulse energy in the experiments is, therefore, probably larger than 1:7, i.e., closer to 1:14.6.

4.2.2 Optimal energy ratio between the pulses. A rule of thumb to find an appropriate energy ratio between the pulses is that the pressure inside the pre-pulse bubble should reach the hydrostatic pressure just after application of the ablation pulse. In this case, the ablation pulse creates no additional force which could result in a dilatation of the vessel wall. In the numerical calculations, this is the case when the equilibrium radius after the ablation pulse equals the maximal radius of the pre-pulse bubble (Fig. 3c). This case corresponds to an energy ratio of 1:14.6. It may well be, however, that even higher energy ratios are applicable. At a ratio of 1:36, the pressure inside the bubble is raised to 0.3 MPa (Fig. 4b), but that may still be tolerable, because in balloon angioplasty even higher pressures are applied for a much longer time. The numerical calculations can, in any case, only be a guideline in finding the optimal energy ratio, since they do not refer to the energy delivered at the fiber tip, but to the fraction of this energy resulting in evaporation, which is not easily measurable. Further experiments are required to find the optimal energy ratio under clinical conditions. We can conclude, however, that pre-pulses with fairly small energy may already reduce the deleterious effects of cavitation considerably.

4.2.3 Optimal timing. The ablation pulse should ideally be applied when the pre-pulse bubble is maximally expanded. To determine the corresponding time delay between the pulses, the oscillation period T of the pre-pulse bubble alone must be known. T can be measured by determining the time difference between the acoustic transients from the bubble generation and the bubble collapse [32]. The optimal delay between the pulses in then $T/2$. The existence of a bubble at the fiber tip can also be detected by monitoring the light reflection of a probe laser beam at the fiber tip. Gas in front of the tip instead of liquid will enlarge the refractive-index difference and thus increase the intensity of the reflected light. As long as the ablation pulse is fired into the expanded pre-pulse bubble, the time delay between the two pulses is not very critical (Figs. 5, 9). The time window during which a volume reduction by a factor of 8 is achieved consists of more than 50% of the oscillation period of the bubble.

4.2.4 Laser system and pulse duration. The double-pulse concept is, of course, not restricted to the combination of lasers used in our experiments, but can be realised with any short-pulse laser. The ablation pulse should ideally be short enough to provide inertial confinement conditions (duration of the laser pulse less than the pressure-dissipation time out of the optical penetration zone) because in this case, the ablation threshold is considerably decreased [33]. On the other hand, it has to be long enough to allow delivery of the pulses without damage to the fiber optics.

The cavitation-bubble dynamics induced by free-running laser pulses resembles the dynamics after double pulses in that early spikes of the pulse train create a cavity into which the ablation products of later spikes can evaporate. Correspondingly, the generation of a cavitation bubble of a given size needs approximately 10 times more energy with a free-running holmium laser than with the excimer laser [5]. Ablation of plaque using free-running holmium-laser pulses of 250–500 μs duration requires, on the other hand, a much higher pulse energy than ablation with excimer-laser pulses having a pulse duration below 200 ns [34]. This disadvantage of free-running pulses is avoided by the use of double pulses with microsecond or submicrosecond duration.

4.2.5 Additional advantages of the double-pulse technique. The displacement of the blood by the pre-pulse increases the energy transmission to the ablation site and provides conditions for the ablation products to move easily away from the ablation site [24]. These effects may improve the ablation efficiency. The wall of the ablated channel is smoother after ablation in gas than in water. In 1985, Grundfest et al. [35] reported that 308 nm excimer-laser pulses applied in an air environment removed atherosclerotic plaque almost without adjacent tissue damage. Displacement of blood from the ablation site by the pre-pulses creates, furthermore, improved conditions for a spectroscopic analysis of the tissue in the vicinity of the fiber tip [36–39]. Identification of normal and atherosclerotic tissue by fluorescence spectroscopy may guide plaque ablation in the case of total vessel occlusion that cannot be crossed by a guide wire [34]. With improved control over the ablation procedure, it may also be possible to create a larger lumen during recanalization of the vessel without risking a perforation of the vessel walls. This would increase the number of cases where laser angioplasty can be performed without adjunctive balloon angioplasty, which is at present often necessary to enlarge the vessel lumen.

5 Conclusions

Cavitation-induced dilatation of the vessel walls occurring in pulsed laser angioplasty can be prevented by dividing the laser pulse energy into a pre-pulse with low energy and an ablation pulse with higher energy. The double-pulse concept may work with an energy ratio of up to about 1:30 between the two pulses. According to the numerical calculations, maximal reduction of the bubble size can be achieved for an energy ratio of about 1:15. The bubble volume is, in this case, reduced by a factor of 17.7 compared to the bubble size occurring after a single pulse of the same energy. The ablation pulse should be applied when the bubble produced by the pre-pulse is maximally expanded. For clinically relevant pulse energies, this is approximately 50–100 μs after the release of the pre-pulse. This time is not very critical, however, because the pre-pulse bubble is close to its maximal size during about 50% of its oscillation cycle. The light transmission to the ablation site is increased, and the ablation efficiency may be improved. Spectroscopic identification of the tissue at the fiber tip is facilitated. The reduction of mechanical collateral effects in combination with a better control over the ablation procedure may lead to a considerable improvement of laser angioplasty or any other technique in laser surgery where ablation has to be performed in a liquid environment.

References

1. A. Vogel, P. Schweiger, A. Frieser, M.N. Asiyo, R. Birngruber: IEEE J. QE-**26**, 2240 (1990)
2. A. Vogel, S. Busch, K. Jungnickel, R. Birngruber: Lasers Surg. Med. **15**, 32 (1994)
3. T. van Leeuwen, M.J. van der Veen, R.M. Verdaasdonk, C. Borst: Lasers Surg. Med. **11**, 26 (1991)
4. M.B. Preisack, W. Neu, R. Nyga, M. Wehrmann, K.K. Haase, K.R. Karsch: Lasers Surg. Med. **12**, 520 (1992)
5. T.G. van Leeuwen, L. van Erven, J.H. Meertens, M. Motamedi, J.M. Post, C. Borst: J. Am. Coll. Cardiol. **19**, 1610 (1992)
6. T.G. van Leeuwen, J.H. Meertens, E. Velema, M.J. Post, C. Borst: Circulation **87**, 1258 (1993)
7. G. Lee, D.T. Mason: Am. J. Cardiol. **69**, 1640 (1992)
8. J.A. Bittl, T.A. Sanborn: Circulation **86**, 71 (1992)
9. A.B. Buchwald, G.S. Werner, C. Unterberg, E. Voth, H. Kreuzer, V. Wiegand: Am. Heart J. **123**, 878 (1992)
10. G.S. Reeder, J.F. Bresnahan, D.R.J. Holmes, F. Litvack: Cathet. Cardiovasc. Diagn. **25**, 195 (1992)
11. T.A. Fischell, M.L. Stadius: Cathet. Cardiovasc. Diagn. **22**, 205 (1991)
12. F. Nakamura, J. Kvasnicka, Y. Uchida, H.J. Geschwind: Am. Heart J. **124**, 1467 (1992)
13. F. Litvack, N.L. Eigler, J.S. Forrester: Circulation **87**, 1421 (1993)
14. J.E. Tcheng, H.R. Phillips, L.D. Wells, R.A. Golobic, J.A. Power, L.I. Deckelbaum: J. Am. Coll. Cardiol. **21**, 386A (1993)
15. M. Oberhoff, S. Hassenstein, H. Hanke, D.Y. Xie, E. Blessing, A. Baumbach, S. Hanke, K.K. Haase, E. Betz, K.R. Karsch: Circulation **86**, 800 (1992)
16. F.R. Gilmore: Calif. Inst. Techn. Rep. **26–4** (1952)
17. R.T. Knapp, J.W. Daily, F.G. Hammitt: *Cavitation* (McGraw-Hill, New York 1971) pp. 117–131
18. K.J. Ebeling: Acustica **40**, 229 (1978) (in German)
19. U. Grigull, J. Straub, P. Schiebner (eds.): *Steam Tables in SI-Units*, 3rd edn. (Springer, Berlin, Heidelberg 1990)
20. L.F. Shampine, M.K. Gordon: *Computer Solution of Ordinary Differential Equations. The Initial Value Problem* (Freeman, San Francisco 1975)
21. Y.C. Fung: *Biomechanics – Mechanical Properties of Living Tissues*, 2nd edn. (Springer, Berlin, Heidelberg 1993)
22. A. Vogel, W. Lauterborn: J. Acoust. Soc. Am. **84**, 719 (1988)
23. R.O. Esenaliev, A.A. Oraevsky, V.S. Letokhov, A.A. Karabutov, T.V. Malinsky: Lasers Surg. Med. **13**, 470 (1993)
24. R.S. Dingus: SPIE Proc. **1646**, 266 (1992)
25. P. Teng, N.S. Nishioka, R.R. Anderson, T.F. Deutsch: IEEE J. QE-**23**, 1845 (1987)
26. R. Fabbro, J. Fournier, P. Ballard, D. Deveaux, J. Virmont: J. Appl. Phys. **68**, 775 (1990)
27. A.G. Doukas, D.J. McAucliffe, T.J. Flotte: Ultrasound Med. Biol. **19**, 137 (1993)
28. M. Delius: Shock Waves **4**, 55 (1994)
29. M.G. Sirotyuk: In *High Intensity Ultrasonic Fields*, ed. by L.D. Rozenberg (Plenum, New York 1971) pp. 263–346
30. G. Paltauf, E. Reichel, H. Schmidt-Kloiber: SPIE Proc. **1646**, 343 (1992)
31. S.L. Jacques, G. Gofstein, R.S. Dingus: SPIE Proc. **1646**, 284 (1992)
32. A. Vogel, W. Hentschel, J. Holzfuß, W. Lauterborn: Ophthalmol. **93**, 1259 (1986)
33. D. Albagli, L.T. Perelman, G.S. Janes, C. von Rosenberg, I. Itzkan, M.S. Feld: Lasers Life Sci. **6**, 55 (1994)
34. L.I. Deckelbaum: Lasers Surg. Med. **14**, 101 (1994)
35. W.S. Grundfest, F. Litvack, J.S. Forrester, T. Goldenberg, H.J.C. Swan, L. Morgenstern, M. Fishbein, I.S. McDermid, D.M. Rider, T.J. Pacala, J.B. Laudenslager: J. Am. Coll. Cardiol. **5**, 929 (1985)
36. G. Laufer, G. Wollenek, K. Hohla, R. Horvat, K.H. Henke, M. Buchelt, G. Wutzl, E. Wolner: Circulation **78**, 1031 (1988)
37. M. Scheu, H. Kagel, M. Zwaan, A. Lebeau, R. Engelhardt: Lasers Surg. Med. **11**, 133 (1991)
38. T.J. Garrand, M.L. Stetz, K.M. O'Brien, G.R. Gindi, B.E. Sumpio, L.I. Deckelbaum: Lasers Surg. Med. **11**, 106 (1991)
39. M. Scheu, R. Engelhardt: SPIE Proc. **1425**, 63 (1991)